Steady state fluorescence technique for studying phase transitions in PAAm–PNIPA mixture

G.A. Evingür , D.K. Aktaş & Ö. Pekcan

Steady state fluorescence technique for studying phase transitions in PAAm–PNIPA mixture

G.A. Evingür[a], D.K. Aktaş[a] and Ö. Pekcan[b]*

[a]*Department of Physics, Istanbul Technical University, Maslak-Istanbul, Turkey;*
[b]*Kadir Has University, Cibali 34230, Istanbul, Turkey*

The *steady state* fluorescence (SSF) technique was used to study the sol-gel phase transition during free radical crosslinking copolymerisation of various amounts of acrylamide (AAm) and *N*-isopropylacrylamide (NIPA) mixtures. N,N'-methylenebis (acrylamide) (BIS) and ammonium persulfate (APS) were used as crosslinker and an initiator, respectively. Pyranine (8-hydroxypyrene-1, 3, 6-trisulfonic acid, trisodium salt, HPTS) was added as a fluoroprobe for monitoring the polymerisation. It was observed that pyranine molecules bind to AAm and NIPA chains upon the initiation of the polymerisation, thus the fluorescence spectra of the bonded pyranines shift to the shorter wavelengths. Fluorescence spectra from the bonded pyranines allowed us to monitor the sol-gel phase transition, without disturbing the system mechanically, and to test the universality of the sol-gel transition as a function of polymer concentration ratios. Observations around the gel point of PAAm–PNIPA mixtures show that the gel fraction exponent β obeyed the percolation result.

Keywords: acrylamide-NIPA; mixture; hydrogel; percolation; critical phenomena; fluorescence

1. Introduction

Hydrophilic gels called hydrogels are important materials for both fundamental and technological interest [1]. Polyacrylamide (PAAm) hydrogels are mainly produced by free radical crosslinking copolymerisation (FCC) of AAm in the presence of N,N'-methylenebis (acrylamide) (BIS) as the crosslinker. Since the monomers are solid at the polymerisation temperature, the reactions are necessarily carried out in an aqueous solution of the monomers. On the other hand, poly(*N*-isopropylacrylamide) (PNIPA) gel is a typical temperature-sensitive gel exhibiting volume phase transition at $\approx 34°C$ [2,3]. The temperature sensitivity of PNIPA gels has been studied both for its fundamental interest and technological application [4–7]. These materials are useful for drug delivery systems, separation operations in biotechnology, processing of agricultural products, sensors, and actuators.

---

*Corresponding author. Email: pekcan@isikun.edu.tr

Hydrogels have received considerable attention for the sol-gel phase transition process. The exact solution of the sol-gel phase transition was first given by Flory and Stockmayer [8,9] on a special lattice called Bethe lattice on which the closed loops were ignored. An alternative to the chemical-kinetic theory is the lattice percolation model [10,11] where monomers are thought to occupy the sites of a periodic lattice. A bond between these lattice sites is formed randomly with probability p. For a certain bond concentration p_c, defined as the percolation threshold, the infinite cluster starts to form in the thermodynamic limit. This is called the percolation cluster in polymer language. The polymeric system is in the sol state below the percolation threshold, p_c.

The predictions of these two theories about the critical exponents for the sol-gel phase transition are different from the point of the universality. Consider, for example, the exponents γ and β for the weight average degree of polymerisation, DP_w, and the gel fraction G, (average cluster size, S_{av}, and the strength of the infinite network P_∞ in percolation language) near the percolation threshold, are defined as:

$$DP_w \propto (p_c - p)^{-\gamma}, \quad p \to p_c^- \tag{1}$$

$$G \propto (p - p_c)^\beta, \quad p \to p_c^+ \tag{2}$$

where the Flory–Stockmayer theory (so-called the classical or mean-field theory) gives $\beta = \gamma = 1$, independent of the dimensionality while the percolation studies based on computer simulations give γ and β around 1.7 and 0.43 in three dimensions, respectively [10–15].

These two universality classes for gelation problem are separated by a Ginzburg criterion [16] that depends upon the chain length N between the branch points as well as the concentration of the nonreacting solvent. The vulcanisation of long linear polymer chains (large N) belongs to the mean-field class. Critical percolation (small N) describes the polymerisation of small multifunctional monomers [10–13].

Experimental techniques used for monitoring sol-gel transition must be very sensitive to the structural changes, and should not disturb the system mechanically. Fluorescence technique is particularly useful for elucidation of detailed structural aspects of the gels. This technique is based on the interpretation of the change in anisotropy, emission and/or excitation spectra, emission intensity and viewing the lifetimes of injected aromatic molecules to monitor the change in their microenvironment [17–20]. Fluorescence probes can be used in two ways for the studies on polymerisation and gelation. First, one can add a luminescent dye as a probe to the system (extrinsic fluoroprobe). By using this fluoroprobe, it is possible to measure some physical parameters of the polymerizing system, like polarity [21,22], physical aging [23], mobility [24], viscosity [25,26] and hydrophobicity [27]. In the second approach, the fluorophore is covalently attached to the polymer, and serves as a polymer-bond label (intrinsic fluoroprobe) [28], where the polymer fluoroprobe association depends on some factors including Coulombic interactions, the hydrophobicity of the polymer–fluorophore pair, etc. Recent studies in our laboratory, using pyrene as an extrinsic fluoroprobe, showed that the glass transition both for the linear bulk polymer [29] and gels [30–32] could be described by percolation exponents. These studies showed that bulk polymer systems and also their mixtures belong to the same universality class. We also determined the percolation exponents during the sol-gel phase transition in AAm [33] and NIPA [34] hydrogels, using pyranine (a derivative of the pyrene molecule, which has three functional groups) as an intrinsic fluoroprobe. In hydrogels, it is found that the critical exponents did not obey the same universality

class, where the most important factor is the monomer concentration in which the exponents differ drastically from percolation to the classical values. It was shown that the critical exponents agree best with the percolation results for high monomer concentrations (above 1M) but they crossover from percolation to classical (mean-field or Flory–Stockmayer) values when the monomer concentration is lower than 2M [33].

In this work, we aimed to study the FCC of AAm–NIPA mixtures and determine the critical exponents for this mixed systems. Here the total monomer concentration is kept 2M and very small amount of pyranine added to the pre-polymerisation solution presented a spectral shift to the shorter wavelengths upon the initiation of polymerisation. This spectral shift is due to the binding of pyranine to the polymer chains during the AAm–NIPA polymerisation. The pyranine, thus, becomes an intrinsic fluoroprobe while it is extrinsic at the beginning of the reaction. The fluorescence intensity of the pyranine bonded to the strands of the polymers allows one to measure directly the gel fraction near the sol-gel phase transition, and thus the corresponding critical exponent, β.

2. Materials and methods

Mixtures were prepared from various amounts of AAm (Merck) and NIPA (Merck) monomers. The monomer concentrations are given in Table 1. BIS (Merck) dissolving in $25 \times 10^{-6} \, \text{m}^3$ of water in which $10^{-4} \, \text{L}$ of TEMED (tetramethylethylenediamine) was added as an accelerator. The initiator, ammonium persulfate (APS, Merck), was recrystallized twice from methanol. The initiator and pyranine concentrations were kept constant at 7×10^{-3} and $4 \times 10^{-4} \, \text{M}$, respectively, for all experiments. All samples were deoxygenated by bubbling nitrogen for 10 min, just before polymerisation process has started.

The fluorescence intensity measurements were carried out using the Model LS-50 spectrometer of Perkin-Elmer, equipped with temperature controller. All measurements were made at 90° position and slit widths were kept at 5 nm. Pyranine was excited at 340 nm during *in situ* gelation experiments and variation in the fluorescence spectra and emission intensity of the pyranine were monitored as a function of polymerisation time.

3. Results and discussion

The control experiment presented in Figure 1 shows the emission spectra of pyranine dissolved in pure water as a function of pH. At high pH (pH = 9), only 508 nm main peak exists. At low pH (pH = 3), in addition to the main peak at 508 nm a small peak (like a shoulder) appears about 440 nm. By decreasing pH, small peak increases and the main peak disappears. The excited pyranine may decay to its ground state by given fluorescence at 440 nm, or it may dissociate upon deprotonation, depending on the pH of the solution. The excited-state anion may dissipate its energy by fluorescence emission at 508 nm. At a pH > 5, the hydrogen ion concentration is insufficient to reprotonate within its lifetime. Therefore, this figure indicates that the 440 nm peak corresponds to the neutralized pyranines by H^+ ions [33].

The typical fluorescence spectra of pyranine at different stages of the AAm–NIPA copolymerisation are shown in Figure 2. At the beginning of the reaction, only the 508 nm peak exists, then the intensity of the new (short wavelength, around 380 nm) peak started to increase and shifted from 380 to 427 nm as the intensity of the 508 nm peak

G.A. Evingür et al.

Table 1. Experimentally measured parameters for mixtures of Aam–NIPA monomers during their gelation.

| AAm [M]	BIS [M]	NIPA (M)	t_c (s)	C^-/C^+	β
2.0	0.013	0	300 ± 5	1.00	0.92
				0.37	0.50
				0.28	0.55
				0.23	0.52
				0.10	0.52
1.8	0.013	0.2	300 ± 5	1.00	0.85
				0.37	0.52
				0.28	0.55
				0.23	0.55
				0.10	0.46
1.6	0.013	0.4	420 ± 5	1.00	0.75
				0.37	0.63
				0.28	0.66
				0.23	0.65
				0.10	0.70
1.5	0.013	0.5	480 ± 5	1.00	1.06
				0.37	0.63
				0.28	0.60
				0.23	0.61
				0.10	0.56
1	0.013	1	600 ± 5	1.00	0.95
				0.37	0.58
				0.28	0.57
				0.23	0.55
				0.10	0.44
0.5	0.013	1.5	1080 ± 5	1.00	0.88
				0.37	0.40
				0.28	0.32
				0.23	0.33
				0.10	0.34
0.4	0.013	1.6	1500 ± 5	1.00	0.87
				0.37	0.37
				0.28	0.37
				0.23	0.31
				0.10	0.31
0.2	0.013	1.8	1800 ± 5	1.00	0.86
				0.37	0.45
				0.28	0.36
				0.23	0.32
				0.10	0.33
0	0.013	2.0	–	1.00	Opaque
				0.37	
				0.28	
				0.23	
				0.10	
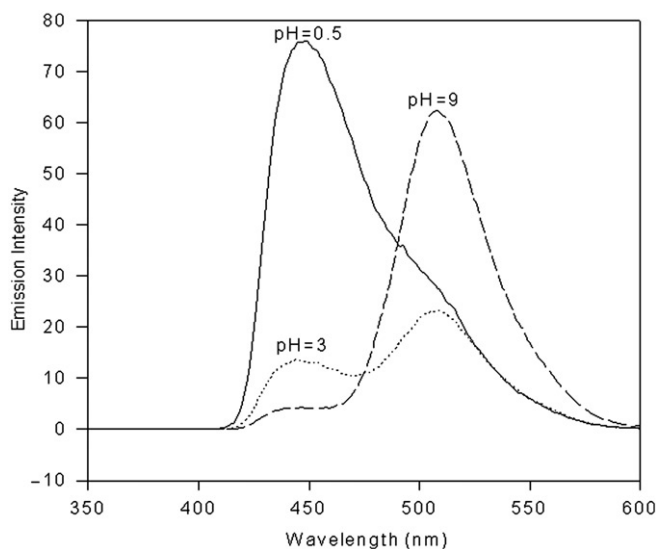
Figure 1. Emission spectra of pyranine dissolved in pure water as a function of pH.
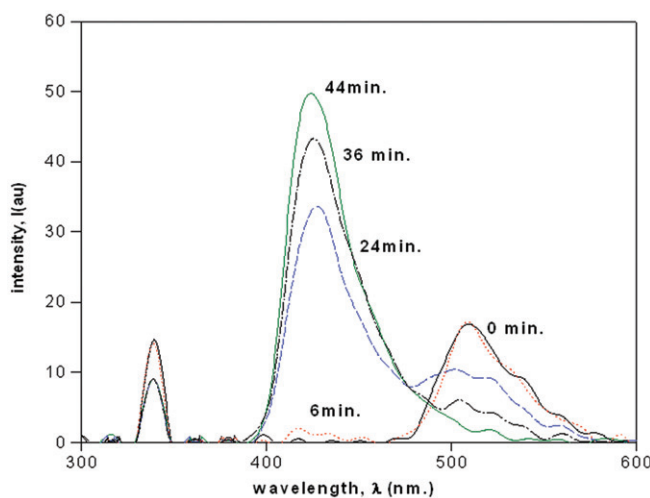

Figure 2. Typical fluorescence spectra of pyranine at different stages during the Aam–NIPA polymerisation. Numbers on the spectra show corresponding reaction times.

(long-wavelength peak) decreased during the course of AAm–NIPA polymerisation. The observations in Figure 2 indicate that the shift in the emission spectra of the pyranine cannot be due to pH effect (shown in Figure 1) since the pH of the reaction did not change considerably during the polymerisation. The shifts in the emission spectra of the pyranine during the polymerisation give more information about the microscopic nature of the polymer–probe interaction, which is defined below as was already described in our previous study [35].

Pyranine is a highly water soluble compound with well-characterized photophysical properties [36]. The chemical structures of pyranine and other monomers used are
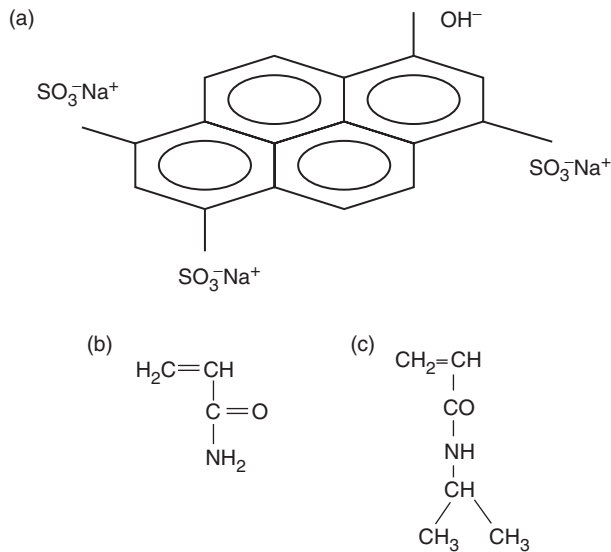
Figure 3. The chemical structures of (a) Pyranine, (b) AAm and (c) NIPA.

shown in Figure 3. Pyranine has three functional groups by which can be bonded to the polymeric network, branched or linear polymers. The probability that pyranine is bonded to the system over more than one functional groups may increase with increasing polymer concentration, and also with the reaction time. As the polymerisation progresses, pyranine can have a chance to bind the polymeric system over two or three functional groups. Here a considerable shift from 508 to 380 nm, as previously observed [35,37], occurs in the emission spectra when –OH group in pyranine binds covalently to a vinyl group of the growing AAm and NIPA polymer chains. At the same time, shift in the short-wavelength peak between 380 and 427 nm is due to binding of SO_3^- groups on pyranine, electrostatically to the AAm and/or NIPA monomers with protonated amide groups either on the same polymer molecule or on the other near polymer strands.

Figure 4 presents the fluorescence intensity of the 508 nm peak, I_{508} (corresponding to free pyranines in the sample cell) from the reaction mixture as a function of the reaction time for different NIPA concentrations. As seen in Figure 4(a) and (b), the fluorescence intensity of the free pyranines first increased then decreased up to some point, and then decreased to zero at the end of the reaction for lower NIPA contents (10% and 25%). For higher NIPA contents (75%) (Figure 4c), the fluorescence intensity of the free pyranines first decreased then increased up to some point again but then not decreased to zero at the end of the reaction. It is seen from Figure 4(c) that there are some unreacted monomers at the end of the reaction as a function of NIPA content.

Figure 5 shows the fluorescence intensities from the bonded pyranine against the reaction time for some different NIPA concentrations. Since the maxima of the spectra, I_{max} (corresponding to bonded pyranine) shifts from 380 to 427 nm as the polymerisation has progressed, one does not have a chance to monitor the intensity in the time drive mode of the spectrometer (10 possible data in 1 s). Therefore, we monitored the fluorescence
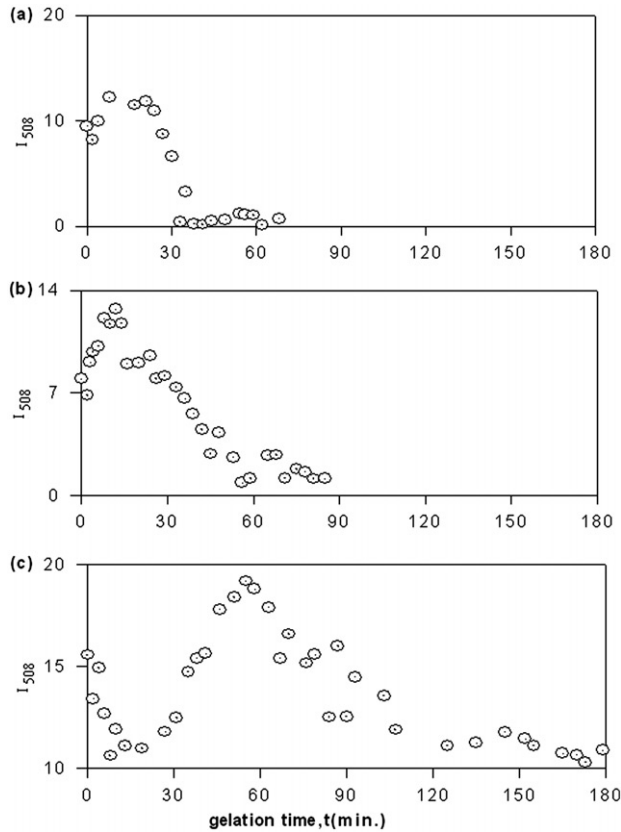
Figure 4. Fluorescence intensity of the free pyranine at 508 nm, I_{508}, *vs*. reaction time for (a) 10% NIPA, (b) 25% NIPA and (c) 75% NIPA concentrations.

spectra in relatively large periods of time and plotted the intensity I_{max} corresponding to the maxima of the spectra as a function of time (Figure 5). We, then, used these data to evaluate the critical behaviour of the sol-gel phase transition.

In order to determine the gel points, t_c, each experiment was repeated at the same experimental conditions, and the gel points were determined by dilatometric technique [38]. A steel sphere of 4.8 mm diameter was moved in the sample up and down slowly by means of a piece of magnet applied from the outer face of the sample cell. The time at which the motion of the sphere is stopped was evaluated as the onset of the gel point, t_c. The t_c values are summarized in Table 1 together with the other parameters.

Here, one would like to argue that the total fluorescence intensity from the bonded pyranines monitors the weight average degree of polymerisation and the growing gel fraction for below and above the gel point, respectively. This proportionality can easily be proven by using a Stauffer type argument [11] as follows, under the assumption that the monomers occupy the sites of an imaginary periodic lattice.

The probability that a site belongs to a cluster of size s is given by $n_s \cdot s$, where n_s is the number of s-cluster (number of clusters including s sites) per lattice site. The probability that an arbitrary site belongs to any cluster is p, this is simply the probability of arbitrary
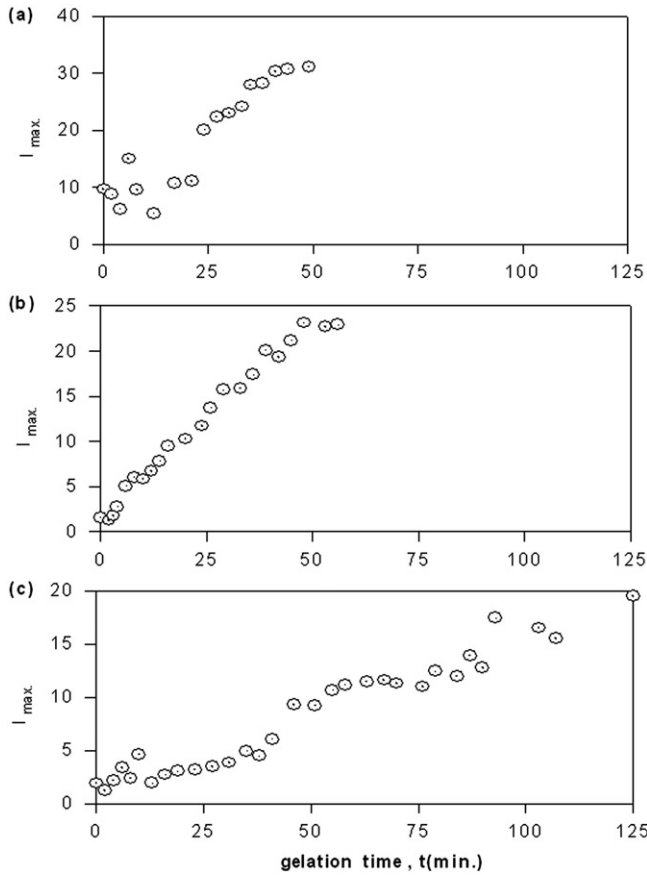
Figure 5. Fluorescence intensity variation of the pyranine, bonded to the gel for (a) 10% NIPA, (b) 25% NIPA and (c) 75% NIPA concentrations, *vs.* reaction time.

site being occupied. Thus, the probability, w_s that the cluster to which an arbitrary occupied site belongs to contains exactly s site is,

$$w_s = \frac{n_s \cdot s}{\sum_s n_s \cdot s} \tag{3}$$

and thus the average cluster size, S is calculated by the following relation [10–13]

$$S = \sum_s w_s \cdot s = \frac{\sum n_s \cdot s^2}{\sum n_s \cdot s} \tag{4}$$

Definition of the average cluster size is the same for all dimensions, although n_s cannot be calculated exactly in higher dimensions [11]. This definition also holds for the bond percolation.

Now, let N_p be the number of pyranine molecules and N_m the other molecules (AAm, NIPA, BIS, water and APS) in the lattice. Thus, the total lattice site, N will be equal to $N_p + N_m$. The probability, P_p, that an arbitrary site is occupied by a pyranine molecule is

simply N_p/N. The probability, P_y, that an arbitrary site both is a pyranine and belongs to the s-cluster, can be calculated as a product of w_s and P_p,

$$P_y = P_p \cdot w_s = \frac{P_p \cdot n_s \cdot s}{\sum n_s \cdot s} \tag{5}$$

Thus, $P_y \cdot s$ will be the total number of pyranine molecules in each cluster including s sites. The total fluorescence intensity, I, which is proportional to the total number of pyranines trapped in the finite clusters, can be calculated as a summation over all s-clusters

$$I \sim \sum_s P_y \cdot s = \sum_s \frac{P_p \cdot n_s \cdot s}{\sum n_s \cdot s} \cdot s = \frac{\sum P_p \cdot n_s \cdot s^2}{\sum n_s \cdot s} \tag{6}$$

where P_p can be taken out of the summation since the concentration of the pyranine is kept fixed for our works,

$$I \sim P_p \frac{\sum n_s \cdot s^2}{\sum n_s \cdot s} = P_p \cdot S \tag{7}$$

Thus, the last expression shows that the total normalised fluorescent intensity, I, is proportional to the average cluster size S. Note that the proportionality factor, P_p is simply the fraction of the pyranine molecules in the sample cell. Intensity will be linearly proportional to the average cluster size, provided that the pyranine concentration is not so high to quench the fluorescence intensity by excitation transfer effect.

Gelation theory often makes the assumption that the conversion factor, p, alone determines the behaviour of the gelation process, though p may depend on temperature, concentration of monomers, and time [10, 11]. If the temperature and concentration are kept fixed, then p will be directly proportional to the reaction time, t. This proportionality is not linear over the whole range of reaction time, but it can be assumed that in the critical region, i.e., around the critical point $|p-p_c|$ is linearly proportional to the $|t-t_c|$ [39, 40].

Therefore, below the gel point, i.e., for $t < t_c$, the maximum fluorescence intensity, $I_{\max}$, measures the weight average degree of polymers (or average cluster size). Above t_c, if the intensity from finite clusters distributed through the infinite network I_{ct} is subtracted from the maximum fluorescence intensity, then, the corrected intensity $I_{\max} - I_{ct}$ measures solely the gel fraction G, the fraction of the monomers that belong to the macroscopic network. In summary, we have the following relations,

$$I_{\max} \propto DP_w = C^+(t_c - t)^{-\gamma}, \quad t \to t_c^- \tag{8a}$$

$$I_{ct} \propto DP_w = C^-(t_c - t)^{-\gamma'}, \quad t \to t_c \tag{8b}$$

$$I_{\max} - I_{ct} \propto G = B(t - t_c)^{\beta}, \quad t \to t_c^+ \tag{9}$$

where C^+, C^- and β are the critical amplitudes.

It is well known that the average cluster size of the finite clusters (distributed through the infinite network) above the gel point decreases with the same, but negative slope of the increasing cluster size below the gel point. This means that the exponents γ and γ', defined for the cluster sizes below and above the gel point, have the same values [10–13]. But, the critical amplitudes for the average cluster size defined below (C^+ in Equation (8a)) and above (C^- in Equation 8b), the gel points are different, and there exist a universal

Table 2. The estimated values for the ratio C^-/C^+.

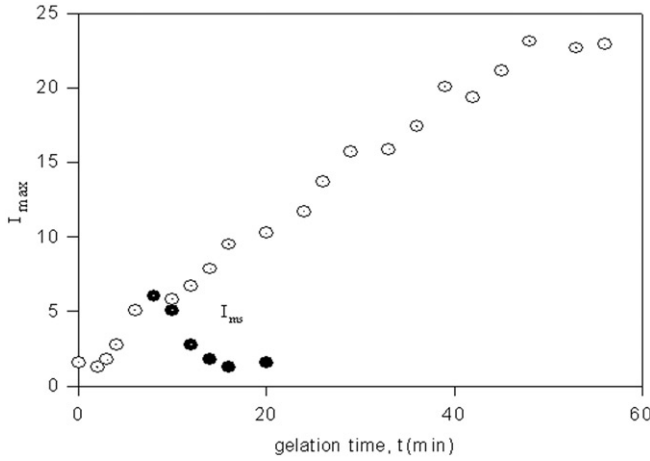|	Classical	Percolation			
		Direct ε expansion	$\gamma_{\varepsilon exp.} = 1.840$ and $\beta_{\varepsilon exp.} = 0.52$	$\gamma = 1.7$ and $\beta = 0.4$	Series and Montecarlo
C^-/C^+	1	0.37	0.28	0.23	0.1

Source: Reference [14].

Figure 6. Intensity-time curve during polymerisation of Aam–NIPA mixture. The curve depicted by dots represents the mirror symmetry I_{ms} of the intensity according to the axis perpendicular to time axis at $t = t_c$. The intensity from the clusters above the gel point is calculated as $I_{ct} = (C^-/C^+)I_{ms}$. Thus, $I_{max} - I_{ct}$ monitors the growing gel fraction for $t > t_c$. The intensity from the below part of the symmetry axis monitors the average cluster size for $t < t_c$.

value for the ratio C^+/C^-. This ratio is different for mean-field *versus* percolation as discussed by Aharony [14] and Stauffer [10]. The estimated values for C^+/C^- [10,14] is given in Table 2.

To determine the intensity I_{ct} in Equations (8b) and (9), we first choose the parts of the intensity-time curves up to the gel points, then the mirror symmetry I_{ms} of these parts according to the axis perpendicular to time axis at the gel point were multiplied by the ratio C^-/C^+, so that $I_{ct} = C^-/C^+ + I_{ms}$. Thus, I_{ct} measures solely the intensity from the cluster above the gel point, and $I_{max} - I_{ct}$ measures the intensity from the gel fraction. This process is clarified explicitly in Figure 6.

Using the Equations (8) and (9), and the values for t_c summarized in Table 1, we calculated β exponents as a function of monomer concentration. Figure 7(a) and (b) represents the log–log plots of the typical intensity-time data above the gel point, for 25% and 50% NIPA concentrations ($C^-/C^+ = 0.28$), respectively, where the slope of the straight lines, close to the gel points, gives β exponents. The produced β values are listed in Table 1 for various monomer contents. On the other hand, γ exponents did not obey any scaling behaviour [34]. Here we have to note that β exponents as seen in Table 1 strongly support that AAm–NIPA mixtures during gelation obey the percolation picture.
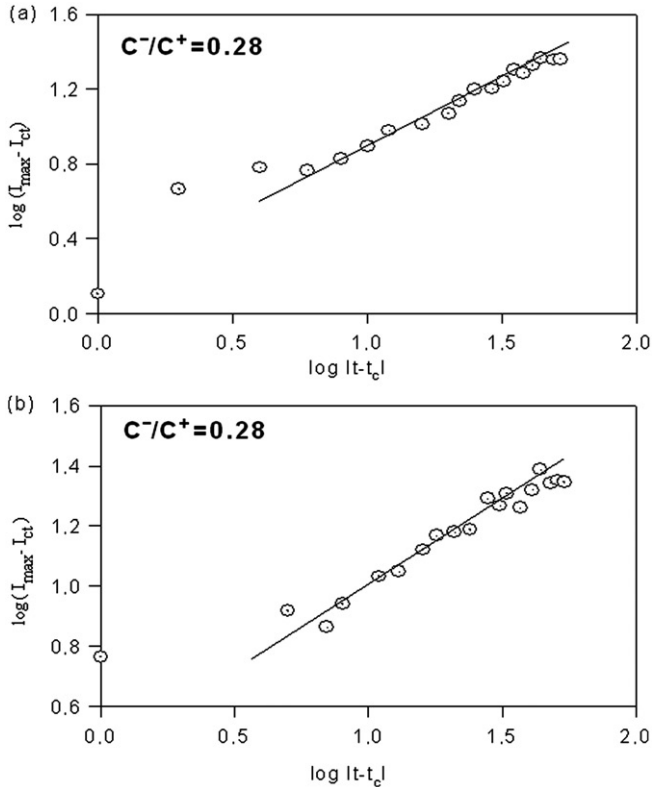
Figure 7. Double logarithmic plot of the intensity $I_{\max} - I_{ct}$ *vs.* time curves above t_c for (a) 25% NIPA and (b) 50% NIPA concentration, respectively (where $C^-/C^+ = 0.28$). The β exponents were determined from the slope of the straight lines.

In conclusion, this work has presented a study of the FCC of AAm–NIPA mixture systems where the critical exponents were determined on the view of universality. Our previous studies showed that the produced critical exponents did not obey the same universality class for AAm [33] and NIPA [34] hydrogels, while bulk gels [30–32] were modeled by percolation picture. In AAm hydrogels, it was shown that the critical exponents agree best with the percolation results for higher AAm concentrations above 1 M, but they crossover from percolation to classical (mean-field or Flory–Stockmayer) values when the AAm concentration goes from 2 M to lower values down to 1M, and present classical values below 1 M. Further down, below 0.5 M, however, no gelation was observed [33]. On the other hand, in NIPA hydrogels [34] the monomer concentration was chosen as 1 M to prevent the system from opacity for various crosslinker contents and the produced exponents were found to agree with the classical results. In the present work, the critical exponents of AAm–NIPA mixture hydrogels were investigated for various monomer concentrations and observed that the gel fraction exponent β agrees best with the percolation theory for various amounts of PAAm–NIPA mixtures. We were, thus, able to measure the copolymerisation kinetics obeying the percolation picture without disturbing the system mechanically. In the mean time, the universality of the sol-gel transition was tested as a function of parameters like polymer concentration ratios.

Here, we have to mention that the meaning of percolation is differing much from the bulk systems [30–32], where the glassy regions percolate.

In future, we plan to study sol-gel phase transition and critical behaviours for other mixed polymeric systems by using fluorescence technique, which allow us to investigate the molecular mechanisms during gelation.

References

[1] T. Tanaka, *Gels*, Sci. Am. 244 (1981), pp. 124–136.
[2] Y. Hirokawa and T. Tanaka, *Volume phase transition in a nonionic gel*, J. Chem. Phys. 81 (1984), pp. 6379–6380.
[3] S. Hirotsu, *Coexistence of phases and the nature of first-order phase transition in poly-N-isopropylacrylamide gels*, Adv. Polym. Sci. 110 (1993), pp. 1–26.
[4] Y.H. Bae, T. Okano, R. Hsu, and S.W. Kim, *Thermo-sensitive polymers as on-off switches for drug release*, Die Makromol. Chem. Rapid Com. 8 (1987), pp. 481–485.
[5] L.C. Dong and A.S. Hoffman, *Thermally reversible hydrogels: III. Immobilisation of enzymes for feedback reaction control*, J. Cont. Release. 4 (1986), pp. 223–227.
[6] R.F.S. Freitas and E.L. Cussler, *Temperature sensitive gels as extraction solvents*, Chem. Eng. Sci. 42 (1987), pp. 97–103.
[7] T. Okano, *Molecular design of temperature-responsive polymers as intelligent materials*, Adv. Polym. Sci. 110 (1993), pp. 179–197.
[8] P.J. Flory, *Molecular size distribution in three dimensional polymers*. *I. Gelation* J. Am. Chem. Soc. 63 (1941), pp. 3083–3090; *Molecular size distribution in three dimensional polymers*. II. Trifunctional branching units, 63 (1941), pp. 3091–3096; *Molecular size distribution in three dimensional polymers*. III. Tetrafunctional branching units. 63 (1941), pp. 3096–3100.
[9] W. Stockmayer, *Theory of molecular size distribution and gel formation in branched-chain polymers*, J. Chem. Phys. 11(1943), pp. 45–54; *Theory of molecular size distribution and gel formation in branched polymers* II. General cross linking. 12 (1944), pp.125–129.
[10] D. Stauffer, A. Coniglio, and M. Adam, *Gelation and critical phenomena*, Adv. Polym. Sci. 44 (1982), pp. 103–158.
[11] D. Stauffer and A. Aharony, *Introduction to Percolation Theory*, 2nd ed., Taylor and Francis, London (second printing), 1994.
[12] M. Sahimi, *Application of Percolation Theory*, Taylor and Francis, London, 1994.
[13] P.G. de Gennes, *Scaling Concepts in Polymer Physics*, Cornell University Press, Ithaca, 1988.
[14] A. Aharony, *Universal critical amplitude ratios for percolation*, Phys. Rev. B 22 (1980), pp. 400–414.
[15] R.H. Colby, J.R. Gillmor, and M. Rubinstein, *Dynamics of near-critical polymer gels*, Phys. Rev. E 48 (1993), pp. 3712–3716.
[16] C.P. Lusignan, T.H. Mourey, J.C. Wilson, and R.H. Colby, *Viscoelasticity of randomly branched polymers in the vulcanisation class*, Phys. Rev. E 60 (1999), pp. 5657–5669.
[17] G.M. Barrow, *Introduction to Molecular Spectroscopy*, McGraw-Hill, New York, 1962.
[18] J.B. Birks, *Photophysics of Aromatic Molecules*, Wiley Interscience, London, 1970.
[19] D.M. Herculus, *Fluorescence and Phosphorescence Analysis*, Wiley Interscience, New York, 1965.
[20] M.D. Galanin, *Luminescence of Molecules and Crystals*, Cambridge International Science Publishing, Cambridge, 1995.
[21] W.F. Jager, A.A. Volkers, and D.C. Neckers, *Solvatochromic fluorescent probes for monitoring the photopolymerisation of dimethacrylates*, Macromolecules 28 (1995), pp. 8153–8158.
[22] T.C. Schaeken and J.M. Warman, *Radiation-induced polymerisation of a mono- and diacrylate studied using a fluorescent molecular probe*, J. Phys. Chem. 99 (1995), pp. 6145–6151.

[23] J.S. Royal and J.M. Torkelson, *Physical aging effects on molecular-scale polymer relaxations monitored with mobility-sensitive fluorescent molecules*, Macromolecules. 26 (1993), pp. 5331–5335.

[24] K.E. Miller, R.H. Krueger, and J.M. Torkelson, *Mobility-sensitive fluorescence probes for quantitative monitoring of water sorption and diffusion in polymer coatings*, J. Polym. Sci. B 33 (1995), pp. 2343–2349.

[25] R. Vatanparast, S. Li, K. Hakala, and H. Lemmetyinen, *Monitoring of curing of polyurethane polymers with fluorescence method*, Macromolecules. 33 (2000), pp. 438–443.

[26] J.M. Warman, R.D. Abellon, H.J. Verhey, J.W. Verhoeven, and J.W. Hofstraat, *Maleimido-fluoroprobe: a dual-purpose fluorogenic probe of polymerisation dynamics*, J. Phys. Chem. B 101 (1997), pp. 4913–4916.

[27] Ş. Erçelen, A.S. Klymchenko, and A.P. Demchenko, *Ultrasensitive fluorescent probe for the hydrophobic range of solvent polarities*, Analytica Chimica Acta. 464 (2002), pp. 273–287.

[28] W.F. Jager, A.M. Sarker, and D.C. Neckers, *Functionalized 4-(Dialklamino)-4′-nitrostilbenes as reactive fluores probes fluores probes for monitoring the photoinitiated polymerization of MMA*, Macromolecules. 32 (1999), pp. 8791–8799.

[29] D. Kaya and Ö. Pekcan, *Comparison of critical parameters of polymerisation and gelation processes: a fast transient fluorescence study*, Int. J. Modern Phys. B. 19 (2005), pp. 971–987.

[30] D. Kaya, Ö. Pekcan, and Y. Yılmaz, *Fast transient fluorescence technique to study critical exponents at the glass transition*, Phase Transit. 76 (2003), pp. 543–556.

[31] D. Kaya and Ö. Pekcan, *Studying of the critical exponents around the glass transition in bulk polymerisation of ethyl methacrylate by using fluorescence techniques*, Phase Transit. 77 (2004), pp. 359–373.

[32] Ö. Pekcan and D. Kaya, *Universal behaviour of glass transition exponents in various polymeric systems*, Comp. Inter. 12 (2005), pp. 501–521.

[33] D. Kaya, Ö. Pekcan, and Y. Yılmaz, *Direct test of the critical exponents at the sol-gel transition*, Phys. Rev. E 69 (2004), p. 16117 (1–10).

[34] D.K. Aktas and Ö. Pekcan, *Study on critical behaviour in N-isopropyl acrylamide gels by using fluorescence technique*, Phase Transit. 79 (2006), pp. 921–933.

[35] Y. Yılmaz, N. Uysal, D.K. Aktaş, O. Güney, A. Gelir, S. Göğebakan and A. Öner, submitted to Polymer.

[36] M. Ashokkumar and F. Grieser, *Sonophotoluminescence: pyranine emission induced by ultrasound*, Chem. Com. (1998), pp. 561–562.

[37] Y. Yılmaz, *Fluorescence study on the phase transition of hydrogen-bonding gels*, Phys. Rev. E 66 (2002), p. 052801(1–4).

[38] O. Okay, D. Kaya, and Ö. Pekcan, *Free-radical crosslinking copolymerisation of styrene and divinylbenzene: real time monitoring of the gel effect using fluorescence probe*, Polymer. 40 (1999), pp. 6179–6187.

[39] Y. Yılmaz, A. Erzan, and Ö. Pekcan, *Critical exponents and fractal dimension at the sol-gel phase transition via in situ fluorescence experiments*, Phys. Rev. E 58 (1998), pp. 7487–7491.

[40] Y. Yılmaz, A. Erzan, and Ö. Pekcan, *Slow release percolate near glass transition Euro*, Phys. J. E 9 (2002), pp. 135–141.